

Soft-x-ray emission spectroscopy study of the electronic structure of nonstoichiometric silicon nitride

V. Jeyasingh Nithianandam and S. E. Schnatterly

Jesse Beams Laboratory of Physics, University of Virginia, Charlottesville, Virginia 22901

(Received 4 November 1986)

Soft-x-ray emission spectroscopy was used to investigate the electronic structure of nonstoichiometric silicon nitride samples of different compositions. The Si L_{23} x-ray emission spectra from these samples are presented and interpreted using a two-phase linear superposition model for the valence-band region. We assumed a model for the valence-band edge and for the emission in the gap region due to trap states and the Si $2p$ core exciton. The results obtained from these fits are compared with relevant models and other experiments.

INTRODUCTION

Electron-stimulated soft-x-ray emission spectroscopy (SXES) has been used to study the valence-band electronic structure of many materials. The valence-band emission spectrum of a material obtained by SXES is helpful in understanding its optical, electronic transport, and other physical properties. Silicon nitride is used as a refractory ceramic and silicon nitride in thin-film form prepared by chemical vapor deposition (CVD) is used in the solid-state electronics industry. A detailed understanding of the changes in valence-band emission spectra due to composition changes in silicon nitride should be very useful in the study of electronic states at the interfaces of these electronic devices. In this work we report the L_{23} emission spectra of crystalline silicon, six different nonstoichiometric silicon nitride samples, and a nearly stoichiometric thin-film silicon nitride sample prepared by CVD. A comparison of our measured x-ray emission spectra from these samples with a calculated density of states is discussed.

EXPERIMENT

Principle

We used SXES as a probe for gaining information about the electronic structure of nonstoichiometric silicon nitride of different compositions. An electron in the Si $2p$ core level is ionized in the sample by a 3-kV electron beam. An electron from an occupied valence-band state of energy $E(\mathbf{k})$ makes a transition to this core vacancy or hole of energy E_c and the energy released in the transition appears in the form of a soft-x-ray photon of energy $\hbar\omega$. The intensity of soft-x-ray emission in the dipole approximation is given by the expression

$$I(\omega) = B\omega \sum_{\mathbf{k}} |\langle c | \hat{\mathbf{a}} \cdot \nabla | \mathbf{k} \rangle|^2 \delta(E(\mathbf{k}) - E_c - \hbar\omega), \quad (1)$$

where B is a constant and $\hat{\mathbf{a}}$ is a unit vector giving the polarization of the photon and the sum is over all occupied electron states. The dipole transition matrix element

$\langle c | \hat{\mathbf{a}} \cdot \nabla | \mathbf{k} \rangle$ between an occupied electron state $|\mathbf{k}\rangle$ and core state $|c\rangle$ dominates the emission process, and so a core state having an orbital angular momentum l probes $l \pm 1$ like components of the occupied electron states with respect to the emitting site. The core state is deep in the emitting atom with little overlap between core states on neighboring atoms and has a well-defined energy. Ignoring various many-body effects, most of which are weak, the variation of spectral intensity with energy of the emitted x-ray photons is thus expected to reflect the density of states of the occupied electron states of the sample.

Experimental details

The soft-x-ray emission spectrograph used in this work was designed and built in our laboratory and is described in detail elsewhere.¹ The emitted x rays were energy dispersed by a holographically aberration-corrected toroidal grating. These soft-x-ray photons were detected by a photodiode array detector. The specimen carousel was cooled to about 195 K with the help of a closed-cycle helium refrigerator and the pressure in the experimental vacuum chamber was better than 2×10^{-9} torr. The energy resolution of the spectrometer in the silicon L_{23} emission range was about 0.1 eV. Nonstoichiometric silicon nitride samples of different compositions were obtained from the Amoco Research Center in fine powder form. These samples were prepared by a pyrolytic process assisted by a carbon dioxide laser. A uniform layer of the silicon nitride powder of 2–3 μm thickness was spread on top of an indium-coated copper plate about $5 \times 5 \text{ mm}^2$, and the powder layer was anchored well to the indium by applying a pressure of 14 000 lb/in.² using a laboratory hydraulic press. For comparison with these samples a nearly stoichiometric silicon nitride sample prepared by CVD was used. Also a c -Si powder sample made using the same pyrolytic process as for the nonstoichiometric samples was measured.

Data reduction

Our raw L_{23} x-ray emission spectra measured in the energy range 65–110 eV were distorted due to contributions

from fourth and fifth orders of the bright nitrogen K x-ray emission spectrum. We introduced appropriate amplitude and energy scaling factors to the measured third-order nitrogen K emission spectrum and subtracted this from the raw L emission spectra of the silicon nitride samples, and thus removed the unwanted fourth- and fifth-order nitrogen K emission contributions.² These corrected spectra were divided by E^3 and normalized to an area of unity. The vertical axis of the spectra reported in this paper is referred to as the transition density of states (TDOS).

We obtained a self-absorption spectrum in the energy region 98–115 eV for amorphous thin-film silicon nitride by finding the point-by-point intensity ratio of two spectra measured with 1.25 and 3-kV incident electron energies.³ The shape of the self-absorption of this sample agrees with the L_{23} absorption edge of silicon nitride obtained using our inelastic electron scattering spectrometer. The self-absorption spectra evaluated in the same way in this energy region from the powder silicon nitride samples do not show the L_{23} absorption edge clearly. It is as though the mean penetration of the incident beam into the powder samples is nearly voltage independent. In any case the effects of self-absorption in the x-ray emission spectra presented here are small and do not alter any of our conclusions.

RESULTS AND DISCUSSION

Two-phase linear superposition model

The experimental L_{23} valence-band x-ray emission spectra for the c -Si and a - Si_3N_4 samples are presented in Fig. 1. These spectra agree with measurements reported

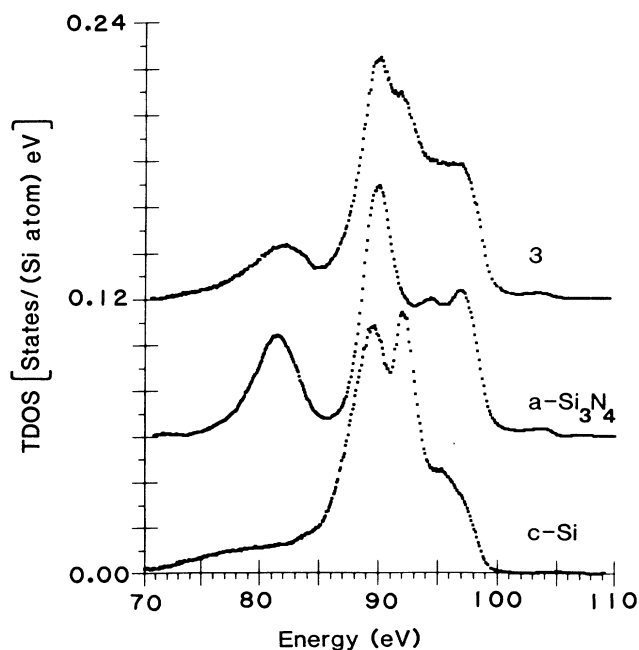


FIG. 1. Si L_{23} emission bands from c -Si, nearly stoichiometric thin-film silicon nitride, and nonstoichiometric silicon nitride sample 3.

in the literature.^{4–9} The spectra from six different nonstoichiometric silicon nitride samples are presented in Fig. 2.

The measured L_{23} x-ray emission spectra from the six nonstoichiometric silicon nitride samples have features which are common to the L_{23} spectra of c -Si and a - Si_3N_4 samples. Moreover, x-ray diffraction and other measurements on SiN_x samples prepared by the CO_2 -laser-assisted pyrolytic process¹⁰ show the coexistence of crystalline and amorphous phases. We therefore assume a linear superposition model to describe the x-ray emission spectra of nonstoichiometric silicon nitride. The physical basis for this model is the assumption that these samples are inhomogeneous, consisting of regions of Si and regions of Si_3N_4 .¹¹ According to this model the transition density of states $\rho(E)$ of these samples is a linear combination of the transition densities of states $\rho_a(E)$ and $\rho_b(E)$ of c -Si and Si_3N_4 , respectively:

$$\rho(E) = A\rho_a(E) + B\rho_b(E). \quad (2)$$

A least-squares curve-fitting program based on Eq. (2) was used to fit each of the L_{23} emission spectra of SiN_x samples with a composite spectrum obtained by a weighted sum of the L_{23} emission spectra of c -Si and a - Si_3N_4 . The adjustable parameters in the program are the weighting factors A and B , and small shifts in the energy axis of component spectra. The reduced χ^2 values for fits to the L_{23} valence-band emission of SiN_x samples based on the two-phase model range between 75 and 406. The values of the parameters obtained from the fits are shown in Table I.

The curve in Fig. 3(b) shows the variation of the reduced χ^2 value of these fits with molar concentration y , where $y = 3x/4$. The model based on Eq. (2) is a macroscopic model that does not take into consideration emissions from states at the interfaces between silicon and silicon nitride regions. We expect therefore that these values of χ^2 are a measure of the number of interface atoms in the samples. Interface disorder will cause scattering of electric states analogous to that in disordered substitutional binary alloys. In that case it is well known that the average scattering power, and hence the resistivity, varies as $y(1-y)$. Our values of χ^2 , shown in Fig. 3(b), peaks near $y = 0.5$ as expected, but the peak is much narrower than that given by this expression. This may indicate a significant interfacial surface tension between the two phases.

Multipeak description of spectra

The x-ray emission spectra of c -Si and the silicon nitride samples do resemble a series of peaks and hence it is tempting to fit them with a small number of broadened line-shape functions. We used a spectral synthesis method in which the shape of the measured spectrum was simulated by a suitable combination of a single line-shape functions. In general, line shapes in x-ray spectra are influenced by the effects of the instrument, lifetime-broadening of the valence and core hole, phonon coupling, and disorder in the sample. We assumed a Voigt profile for our line shape. This results from the convolution of a Lorentzian and a Gaussian line shape. The

Voigt profile is given by

$$H(x,y) = \frac{y}{\pi} \int_{-\infty}^{\infty} \frac{\exp(-t^2)}{y^2 + (x-t)^2} dt, \quad (3)$$

where $x = 2\sqrt{\ln 2}(E - E_0)/\Gamma_g$, and $y = \sqrt{\ln 2} \Gamma_l/\Gamma_g$. E_0 is the center of the peak, Γ_l and Γ_g are the full widths at half maximum (FWHM) of Lorentzian and Gaussian functions. The FWHM of the Voigt profile, Γ_V , can be approximated by

$$\Gamma_V \approx 0.5[\Gamma_l + (\Gamma_l^2 + 4\Gamma_g^2)^{1/2}]. \quad (4)$$

For a spectrum of M overlapping lines, the measured intensity $I(E)$ is given by

$$I(E) = \sum_{i=1}^M N(E_{oi}) H(x_i, y_i), \quad (5)$$

and $N(E_{oi})$ is the intensity of the peak at its center position E_{oi} . In each case we used the smallest number of

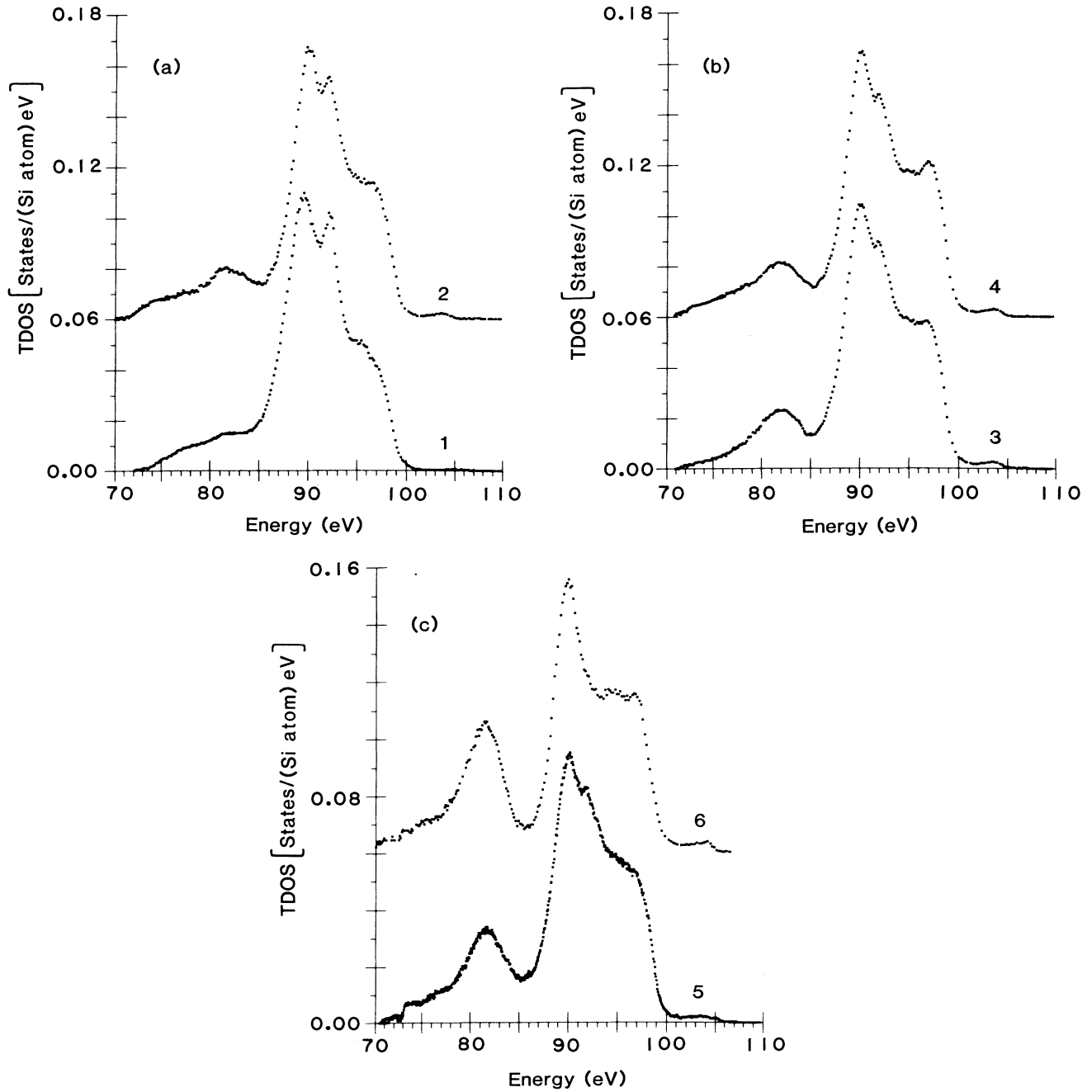


FIG. 2. (a) Si L_{23} emission bands from samples 1 and 2. (b) Si L_{23} emission bands from samples 3 and 4. (c) Si L_{23} emission bands from samples 5 and 6.

TABLE I. Parameters of two-phase model fit to the valence band. A and B are the weighting factors as defined in Eq. (2) and x is the composition index given by $x = 1.3B/(A+B)$.

Sample no.	Weighting factors		Composition x	χ^2 value
	A	B		
1	0.94	0.09	0.11	190.3
2	0.59	0.37	0.5	183.1
3	0.51	0.47	0.63	217.7
4	0.47	0.47	0.65	406.3
5	0.34	0.65	0.86	109.7
6	0.03	0.91	1.26	74.5

components of reasonable FWHM that could produce a good fit to each spectrum. Figure 4 shows a fit to the valence-band emission spectrum of sample 3 with five broadened line-shape functions. Table II shows the parameter values obtained in fitting our spectra in this way. The reduced χ^2 values ranged between 5 and 21. Since these fits are quite good, these parameters provide a convenient way for others to regenerate our results for later comparison with calculations or other measurements.

There are no theoretical electronic structure calculations for nonstoichiometric silicon nitride with different compositions. The L_{23} x-ray emission spectra of c -Si and sample 1 show a shoulder region between 94 and 99 eV and two prominent peaks at lower energies. The general shape of these two spectra are very similar, but there are some significant differences between them. The shoulder region of sample 1 is more intense than the c -Si shoulder region due to additional contributions from N: $2p$ states.¹²⁻¹⁹ There is a small bump at 81.3 eV due to N: $2s$ states¹³ in the spectrum of sample 1. The valence-band emission spectrum of sample 1 was resolved into six components. The intensity of the resolved component at about 92 eV in the spectrum of sample 1 is greater than the corresponding peak of the c -Si spectrum, perhaps due¹²⁻¹⁹ to additional contributions from nitrogen $2p$ states.

Cartling's²⁰ self-consistent-field $X\alpha$ scattered-wave (SCF- $X\alpha$ -SW) molecular-orbital calculation for a cluster of 17 silicon atoms in a simulated crystalline environment yields seven molecular-orbital energy levels: $1a_1$, $1t_2$, $2a_1$, $2t_2$, $1e$, $3t_2$, and $1t_1$. But we obtained good fit to the spectrum of c -Si between 86 and 99 eV with just six Voigt components. A seven-component fit in this energy region gave an additional component at 95.0 eV. The spacings of Cartling's energy levels do not however agree well with the energy positions of the components obtained from our curve-fitting method.

The L_{23} x-ray emission spectra from silicon nitride samples show that the valence band consists of two sub-

bands. Our spectra for samples 2 to 5 show an upper valence band with four discernible peaks. The peak at 92 eV in the spectra apparently due to the presence of c -Si in the samples has not been reported in previous x-ray emission measurements.⁷⁻⁹ Although Robertson's¹³ electronic structure calculation for Si_3N_4 shows four features in the upper valence subband, the positions of these features do not line up with the positions of the four resolved components of our spectrum. Although the spacings of the energy levels do not agree with our measurements, the order of the various features is agreed upon by all present calculations.¹²⁻¹⁹ According to these calculations,^{12,13} peak B is mostly N: $2p_x$ and $2p_y$ with some admixture of Si: $3s$ states. These calculations show that the peaks C and E ^{12,13} have some contributions from Si: $3p$ in addition to N: $2p_x$ and $2p_y$ states and the peak G has contributions from N: $2p_z$ states.

Valence-band edge and gap region

The electronic and optical properties of silicon nitride are associated with the states at the top of the valence band, in the gap region and in the conduction band. We developed a nonlinear least-squares program to fit our measured spectra of silicon nitride samples in the region 98-108 eV which includes the top of the valence band, band-gap region, and the bottom of the conduction band. We briefly outline the basis of our model for this energy region.

We assume a straight line $A_t(E_t - E)$ convoluted with a Gaussian function $\exp[-(E - E_0)/b\Gamma]^2$, where $b = 1/2\sqrt{\ln 2}$ to fit the top of L_{23} valence-band emission spectra. E_t is the position of the top of the valence band and Γ is the FWHM of the Gaussian broadening function. This broadening is probably due to the presence of inequivalent Si sites in the unit cell of silicon nitride as well as disorder. The functional form of our model, $V(E)$, for the L_{23} valence-band edge of silicon nitride is described by the following expression:

$$V(E) = \frac{1}{2}\sqrt{\pi} A_t b \Gamma (E_t - E) \left[\operatorname{erf} \left[\frac{E_t - E}{b\Gamma} \right] + \operatorname{erf} \left[\frac{E}{b\Gamma} \right] \right] + \frac{1}{2} A_t (b\Gamma)^2 \left\{ \exp \left[- \left[\frac{E_t - E}{b\Gamma} \right]^2 \right] - \exp \left[- \left[\frac{E}{b\Gamma} \right]^2 \right] \right\}. \quad (6)$$

The disorder in these amorphous samples introduces potential fluctuations which remove sharp band edges, and a valence-band tail occurs. Robertson^{13,15} concludes that localized states in the valence-band tail could extend up to 1.5 eV into the gap region for silicon nitride and that

these tail states are due to the $\equiv\text{Si}-\text{Si}\equiv$ homopolar unit and $\equiv\text{N}$ centers. Theoretical calculations^{14,15} show that gap states due to $\equiv\text{Si}-\text{Si}\equiv$ units have bonding character and $\equiv\text{Si}$ dangling bonds have antibonding character. Recent investigations on the photolumines-

cence properties²¹ of SiN_x show evidence for the existence of electronic states in the valence-band tail. As is commonly done,²² we assume for the shape of the density of states distribution in the valence-band tail a simple exponential form:

$$G(E) = G_0 \exp \left[- \left(\frac{E - E_t}{W} \right) \right], \quad (7)$$

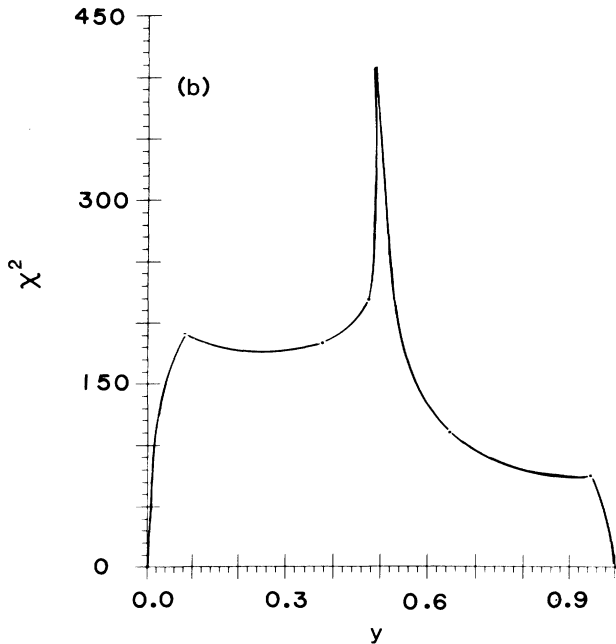
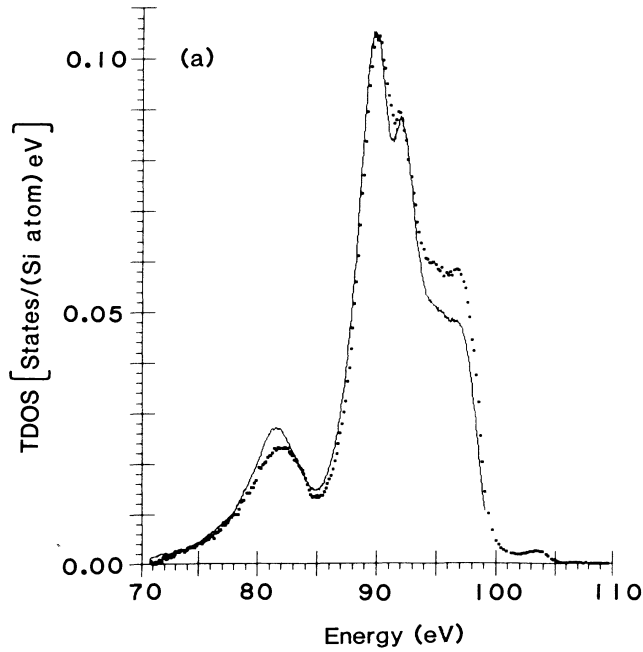


FIG. 3. (a) Fit to the valence-band emission spectrum of sample 3 based on two-phase linear superposition model. (b) Reduced χ^2 value of fits based on Eq. (2) as a function of molar concentration y .

where $G_0 = N_t/W$ is the density of states just above the mobility edge. Here W is the width of the exponential valence-band tail, and N_t is the number density of defect states in the gap. In order to fit our experimental data we convoluted Eq. (7) with a Gaussian broadening function, and the resulting expression for the valence-band tail $T(E)$ is given by

$$T(E) = \frac{1}{2} \sqrt{\pi} G_0 b \Gamma \exp \left[\frac{E_t - E}{W} \right] \exp \left[\left(\frac{b\Gamma}{W} \right)^2 \right] \\ \times \left[\operatorname{erf} \left(\frac{b\Gamma}{W} + \frac{E_m}{b\Gamma} - \frac{E}{b\Gamma} \right) - \operatorname{erf} \left(\frac{b\Gamma}{W} - \frac{E}{b\Gamma} \right) \right] \\ \text{for } E > M, \quad (8)$$

$$T(E) = 0 \text{ for } E < M.$$

E_m is the upper limit of the convolution integral and M presumably corresponds to the mobility edge. The function $T(E)$ is joined to the function $V(E)$ at the mobility edge so as to best fit the data.

The shape and the strength of the emission near the middle of the gap region and near the conduction-band edge changes as the composition index x changes in SiN_x . The emission near the conduction-band edge or L_{23} x-ray absorption edge is due to the Si $2p$ core exciton, and the remaining emission at lower energies in the gap is likely due to $\equiv\text{Si}$ trap states.¹⁵ We assumed Voigt profiles for the core exciton and the $\equiv\text{Si}$ trap states in our model for the gap region.

Our model for the emission in the gap region includes $V(E)$, $T(E)$, and a set of Voigt line-shape functions for the trap states and core exciton. We include the L_2/L_3

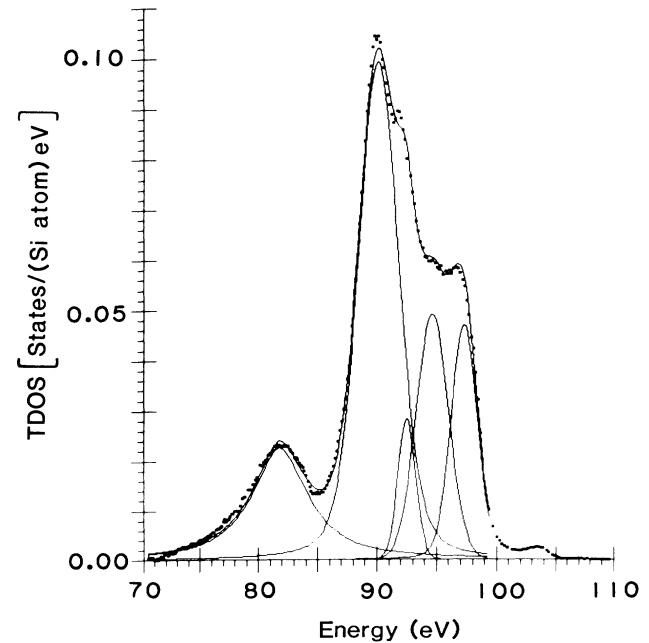


FIG. 4. Fit the valence-band emission spectrum of sample 3 with five broadened line-shape functions.

TABLE II. Parameters of multipeak fit to the valence band. E_{oi} is the energy position of peak and Γ_v is the full width at half maximum of the Voigt profile in eV. $N(E_{oi})$ is the intensity of the peak in transition density-of-states units.

Parameter	Peak	A	B	C	D	E	F	G	χ^2
c-Si									
E_{oi}			89.55	91.84	92.62	94.02	95.84	97.56	
Γ_v			4.98	1.0	1.51	2.26	2.42	1.76	13.2
$N(E_{oi})$			0.10	0.032	0.045	0.023	0.031	0.016	
SiN film									
E_{oi}	81.39	89.81	92.01			94.44		97.24	
Γ_v	4.07	2.78	2.43			3.59		2.52	4.8
$N(E_{oi})$	0.043	0.10	0.022			0.052		0.048	
Sample 1									
E_{oi}	81.25	89.49	92.24			93.78	95.87	97.66	
Γ_v	6.08	4.38	1.62			2.78	2.72	1.81	10.4
$N(E_{oi})$	0.01	0.10	0.048			0.026	0.033	0.019	
Sample 2									
E_{oi}	81.48	89.88	92.23			94.23		97.13	
Γ_v	5.28	3.59	1.64			3.87		2.66	13.8
$N(E_{oi})$	0.017	0.10	0.035			0.044		0.037	
Sample 3									
E_{oi}	81.77	90.12	92.49			94.63		97.29	
Γ_v	5.95	3.98	1.75			3.2		2.57	21.0
$N(E_{oi})$	0.02	0.099	0.028			0.015		0.047	
Sample 4									
E_{oi}	81.64	90.04	92.48			94.92		97.5	
Γ_v	5.61	3.57	2.0			3.4		2.35	16.4
$N(E_{oi})$	0.019	0.099	0.037			0.05		0.046	
Sample 5									
E_{oi}	81.5	89.80	92.27			94.99		97.46	
Γ_v	5.06	3.33	2.55			3.65		2.36	16.4
$N(E_{oi})$	0.03	0.084	0.041			0.048		0.03	
Sample 6									
E_{oi}	81.18	89.84	92.21			94.36		97.1	
Γ_v	4.60	3.11	1.99			3.28		2.68	9.5
$N(E_{oi})$	0.044	0.093	0.02			0.048		0.044	

emission intensity ratio of 0.5, and the 0.61-eV Si 2p spin-orbit splitting. A fit based on this model to the spectrum of sample 3 for states at the top of the valence band and in the gap region is shown in Fig. 5. The values of the parameters of the fits to our data are given in Table III. The reduced χ^2 values for the fits based on our model to the spectra in the gap region lie between 1.3 to 19.0.

The fits to the silicon-rich SiN_x samples show some interesting features. The shape of the emission peak above the top of the valence band of sample 2 was symmetric, and we obtained a good fit to the spectrum of sample 2 in the gap region with just one Voigt profile. The spectra of samples 3–5 in this energy region were not symmetric and we were forced to use two Voigt functions to fit the emission from the occupied gap states. The band due to traps for samples 3 and 4 was found to be at 3.5 eV above

the top of the valence-band edge. The trap state for sample 5 was found to be at 3.2 eV above the top of the valence-band edge. The peaks due to trap states in samples 3–5 are well separated from the exciton states at the bottom of the conduction band by 0.9, 1.1, and 1.6 eV, respectively while the exciton peak in sample 2 merges with the defect states.

Robertson,^{13,15} in his electronic-structure calculations of gap states in silicon nitride obtained the result that the singly occupied $\equiv\text{Si}^0$ gap state or trapped hole level and the doubly occupied $\equiv\text{Si}^-$ state or trapped electron level are at 3.1 and 3.5 eV, respectively, above the top of the valence band. Our emission peaks fall in the range 3.2–3.5 eV above the valence-band top, so it is quite likely that we are seeing emission from these defect states.

The energy separation between the exciton and the im-

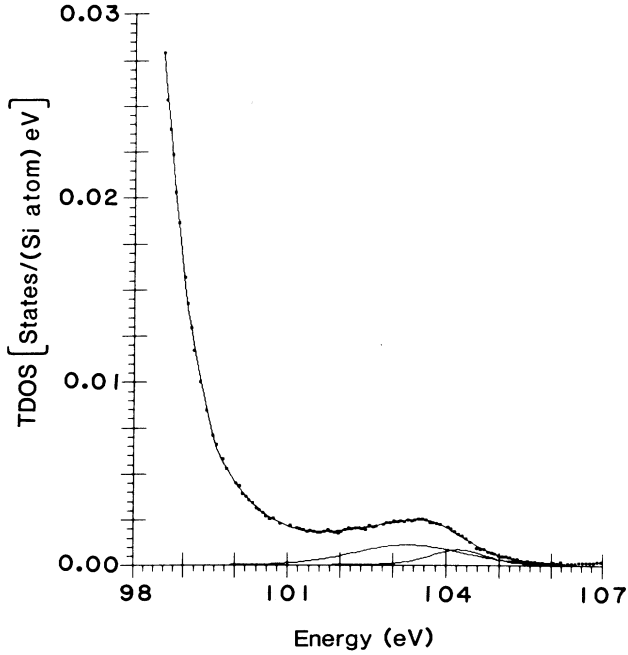


FIG. 5. The valence-band edge and gap region part of the L_{23} emission spectrum of sample 3 and fit based on a model for this region.

purity band increases as the excess silicon content decreases or the value of the composition index x increases. The energy of the exciton peak increases with an increase in the value of x . Thus there is a red shift of the L_{23} absorption edge in SiN_x with the enrichment by excess silicon.²³ The difference in the energy of the position of the top of the valence band and the position of the Si $2p$ core exciton, discounting any change in the exciton binding energy, is a measure of the value of the band gap, and we see that this value steadily increases as the excess silicon content decreases. Following the discussions mentioned above we speculate as follows: The merging of the Si $2p$ core exciton peak with the emission due to $\equiv\text{Si}$ defect states in the spectrum of sample 2 with an estimated composition $x=0.5$, is reminiscent of a transition to the metallic phase in a metal-nonmetal transition and the curves in Fig. 6 representing the position of the exciton peak and the trap peak intersect at composition $x=0.5$. This picture of the localized states merging into the conduction band only makes sense if the sample is fairly homogeneous, i.e., if the two-phase model described above is no longer accurate in this concentration range. Indeed, the reduced χ^2 values in Table I suggest that this may be the case. It is interesting that this merging is roughly consistent with the Mott condition²⁴ $n^{1/3}a_0 \gtrsim 0.26$, where a_0 is the modified Bohr radius. Estimating the number den-

TABLE III. Model parameters for top of valence band and gap region. E_t is the position of the top of the valence band in eV. A_t is slope of the function representing the top of the valence band in units of states/(eV² Si atom). Γ is the full width at half maximum of the Gaussian broadening function in eV. M is the energy position at which the $T(E)$ function joins the $V(E)$ function, and W is the width of the exponential tail in eV. N_t is the number of states/(Si atom) at M .

Sample	SiN film	2	3	4	5	6
Parameter						
			$V(E)$			
E_t	98.98	99.31	99.2	99.08	99.26	98.96
A_t	1.35×10^{-2}	1.77×10^{-2}	2.2×10^{-2}	2.7×10^{-2}	2.01×10^{-2}	1.2×10^{-2}
Γ	1.74	0.83	0.91	1.02	0.84	1.72
			$T(E)$			
M	99.31	99.17	99.06	99.06	99.22	99.12
W	1.31	1.20	1.06	1.1	1.19	1.53
N_t	2.0×10^{-3}	3.36×10^{-3}	4.0×10^{-3}	4.2×10^{-3}	3.9×10^{-3}	2.7×10^{-3}
			Gap states			
E_{oi}	102.48		102.67	102.56	102.45	102.43
Γ_v	2.25		2.45	2.12	2.84	1.84
$N(E_{oi})$	1.4×10^{-3}		1.1×10^{-3}	1.1×10^{-3}	7.0×10^{-4}	1.2×10^{-3}
			Exciton			
E_{oi}	103.74	103.24	103.61	103.62	104.03	103.61
Γ_v	1.02	1.97	1.2	1.23	2.47	1.15
$N(E_{oi})$	1.8×10^{-3}	1.5×10^{-3}	9.0×10^{-4}	1.3×10^{-3}	9.0×10^{-4}	1.4×10^{-3}
χ^2	19.0	5.2	2.7	3.0	6.92	1.3
value						
			Spin-density values			
Spins/cm ³		4.2×10^{18}	1.3×10^{19}		5.4×10^{18}	1.6×10^{18}

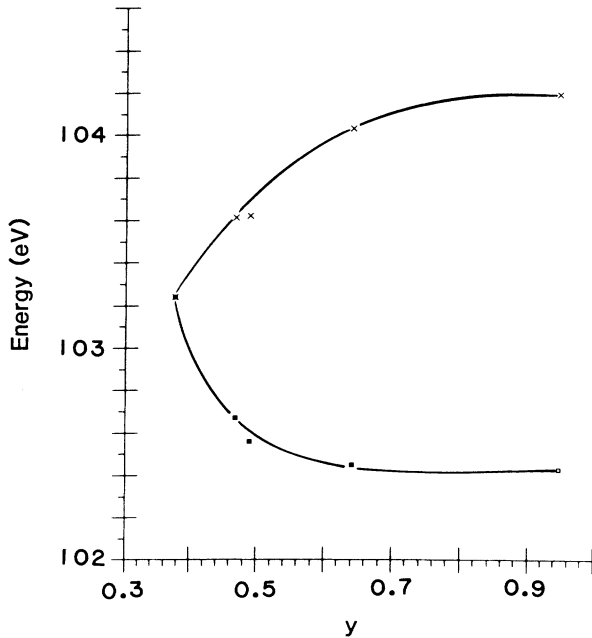


FIG. 6. The upper curve is the position of Si 2*p* core exciton and the lower curve is the peak representing trap states as a function of molar concentration y , where $y = 3x/4$.

sity n from the emission intensity in the gap region we find $n^{1/3}a_0 = 0.46$ for this sample.

The Lorentzian width of the Voigt profile used to fit the Si 2*p* core exciton represents the lifetime broadening of the core and valence hole. The width of the valence-band tail estimated from our fits for the spectra of samples 4–6, increases with the increase in the value of the composition index x . The increase in the width of the valence-band tail and the band gap with the decrease in the silicon content are in agreement with the conclusions from photoluminescence measurements²¹ on nonstoichiometric silicon nitride.

The *L* emission spectrum of sample 6 in the energy region 98 to 108 eV was fit using a Voigt function for the trap states, one more, as shown in Table III, for an $n = 1$ exciton, and another at 104.2 for the $n = 2$ exciton. The reduced χ^2 value for the fit is 1.3. Let us assume that the latter two Voigt functions correspond to the first two exciton lines with $n = 1, 2$ in the excitonic series given by

$$E_n = E_g - \frac{E_x}{n^2}, \quad (9)$$

where E_x is the binding energy of the exciton, E_g is the energy gap, and E_n is the position of exciton lines below the bottom of the conduction band. By fitting both peaks with a Voigt profile, we estimate from the difference in the positions of the two exciton lines the binding energy of Si:2*p* core exciton as 0.8 eV and the band-gap value as 5.4 eV. The composition of this sample from our two-phase model is $x = 1.26$. The optical absorption gives a value of 5.5 eV for the optical gap.²⁵ Ley *et al.*,²⁵ in their work on Fano-type antiresonance below the L_{23} threshold, reported 0.6 and 1.45 eV for the binding energy of a Si:2*p*

core exciton in a-SiN_{*x*}:H with $x = 1.2$ and 1.45, respectively. Hjalmarsen, Butner, and Dow²⁶ in their theoretical calculation have estimated the binding energy of a Si:2*p* Frenkel core exciton in Si₃N₄ as 1.2 eV.

The spin-density values measured by electron spin resonance for some of these SiN_{*x*} samples are given in Table III. Fujita and Sasaki²⁷ show that the memory trap density due to ≡Si dangling bonds in CVD silicon nitride films are larger than the spin-density values, and the relationship between these two quantities is nonlinear. The volume densities obtained from our fit to the DOS for the ≡Si traps range between 4.5×10^{20} and 6.4×10^{20} states/cm³, 1 to 2 orders of magnitude greater than the spin densities, and in reasonable agreement with other results.²⁷

The variation in the energy gap with composition in crystalline semiconductor alloys²⁸ is approximated by a quadratic form:

$$E_g(y) = E_A + ay + by^2, \quad (10)$$

where $a = (E_B - E_A) - b$, y is the molar concentration, and E_A and E_B are the band gaps of the two component semiconductor compounds *A* and *B*. The factor b is called as the bowing parameter, and it is a measure of the nonlinearity of the variation. We assume the position of the Si 2*p* core exciton E_{2pc} above the top of the valence band to be a measure of the band gap. The values of E_{2pc} obtained for different a-SiN_{*x*} samples based on our model in the gap region are given in Table III. We assume that Eq. (10) applies to amorphous semiconductors. We obtained for SiN_{*x*} a fit to the values of E_{2pc} and $y = 3x/4$ based on Eq. (10) and Fig. 7 shows the fit to the data. The values of E_A , a , b , and E_B obtained from the fit are

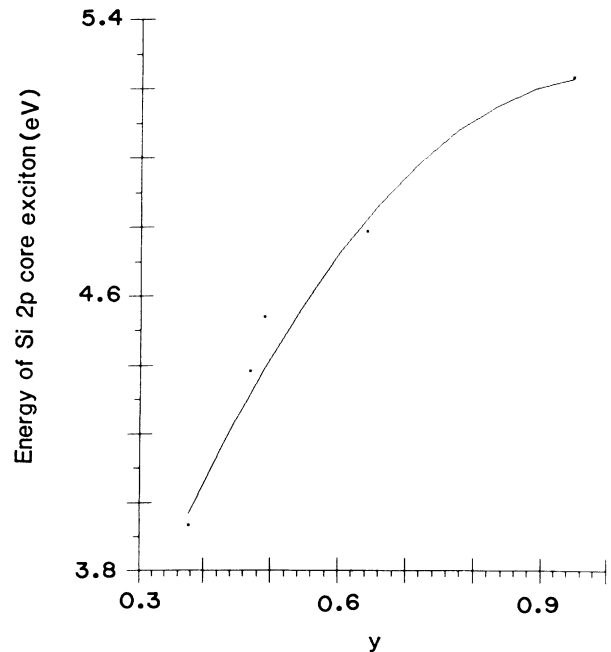


FIG. 7. Position of Si 2*p* core exciton as a function of molar concentration y and a fit based on Eq. (10).

1.95, 6.6, -3.3 , and 5.24 eV, respectively. The fact that the band gap has the expected variation lends credence to the y values obtained from the two-phase model, at least for large y .

SUMMARY AND CONCLUSIONS

We have investigated the electronic structure of SiN_x as a function of excess silicon content using high-resolution soft-x-ray emission spectroscopy. We conclude as follows.

1. The two-phase linear superposition model describes the electronic structure of SiN_x reasonably well. The discrepancies between the two-phase model fits and our spectra for $y > 0.5$ are small and the discrepancies are large for $y < 0.5$ in the nitrogen $2s$ bump region and for the nitrogen $2p_z$ peak region. We obtained reasonable values for the composition x for our samples from these fits.

2. Our assumed model for the top of the valence band and the gap region gave good fits to our spectra for $y > 0.1$. We estimated the number of electronic states per cm^3 due to defect states in the gap.

3. We conclude on the basis of the energy of the Si $2p$ Frenkel core exciton that there is a red shift of the L_{23} absorption edge in SiN_x with the enrichment by excess silicon.

4. The shape of the emission in the gap region changes

drastically as the composition changes. The intensity is minimum for $y=0.6$ and the shape of the emission for $y=0.95$ is asymmetric near the L_{23} absorption threshold. The shape of the emission is symmetric for $y=0.4$ and the $\equiv\text{Si}$ defect states merge with the Si $2p$ core exciton, reminiscent of a transition between metallic and nonmetallic behavior.

5. We obtained the binding energy of the Si $2p$ Frenkel core exciton as 0.8 eV for the composition $x=1.26$. The width of the core exciton changes with composition and it has a maximum value for $y=0.7$.

6. The band gap increases with the decrease of excess silicon content, and the width of the exponential tail increases for $y > 0.49$.

ACKNOWLEDGMENTS

The authors wish to thank Dr. F. Chambers of Amoco Research Center for the silicon nitride samples and the spin-density values. The authors also acknowledge the other members of our group, R. D. Carson, P. Livins, P. Bruhwiler, D. Husk, C. Tarrio, and A. Mansour, as well as Dr. B. Abeles of Exxon, for their help and useful discussions throughout the course of this work. This work was supported in part by National Science Foundation Grant No. 85-15684.

¹R. D. Carson, C. P. Frank, S. E. Schnatterly, and F. Zutavern, *Rev. Sci. Instrum.* **55**, 1973 (1984).

²R. D. Carson and S. E. Schnatterly, *Phys. Rev. B* **33**, 2432 (1986).

³R. J. Liefeld, in *Soft X-ray Band Spectra*, edited by D. J. Fabian (Academic, London, 1968), p. 133.

⁴E. Z. Kurmaev and G. Weich, *J. Non-Cryst. Solids* **70**, 187 (1985).

⁵Z. A. Weinberg and R. A. Pollak, *Appl. Phys. Lett.* **27**, 254 (1975).

⁶R. Karcher, L. Ley, and R. L. Johnson, *Phys. Rev. B* **30**, 1896 (1984).

⁷I. A. Brytov, V. A. Gritsenko, Yu. P. Kostikov, E. A. Obolenski, and Yu. N. Romashchenko, *Fiz. Tverd. Tela (Leningrad)* **26**, 1685 (1984) [*Sov. Phys.—Solid State* **26**, 1022 (1984)].

⁸I. I. Zhukova, V. A. Fomichev, A. S. Vinogradov, and T. M. Zimkina, *Fiz. Tverd. Tela (Leningrad)* **10**, 1383 (1968) [*Sov. Phys.—Solid State* **10**, 1097 (1968)].

⁹I. A. Brytov, E. A. Obolenski, Yu. N. Romashchenko, and V. A. Gritsenko, *J. Phys. (Paris) Colloq.* **2**, C887 (1984).

¹⁰Y. Kizaki, T. Kandori, and Y. Fujitani, *Jpn. J. Appl. Phys. Part 1* **24**, 800 (1985).

¹¹E. A. Irene, N. J. Chou, D. W. Dong, and E. Tierney, *J. Electrochem. Soc.* **127**, 2518 (1980).

¹²E. C. Ferreira and C. E. T. Goncalves da Silva, *Phys. Rev. B* **32**, 8332 (1985).

¹³J. Robertson, *Philos. Mag. B* **44**, 215 (1981).

¹⁴G. Lucovsky and S. Y. Lin, *J. Vac. Sci. Technol. B* **3**, 1122 (1985).

¹⁵J. Robertson and M. J. Powell, *Appl. Phys. Lett.* **44**, 415 (1984).

¹⁶J. Robertson, *J. Appl. Phys.* **54**, 4490 (1983).

¹⁷R. J. Sokel, *J. Phys. Chem. Solids* **41**, 899 (1980).

¹⁸S. Y. Ren and W. Y. Ching, *Phys. Rev. B* **23**, 5454 (1981).

¹⁹A. G. Petukhov, *Fiz. Tverd. Tela (Leningrad)* **27**, 95 (1985) [*Sov. Phys.—Solid State* **27**, 55 (1985)].

²⁰Bo. G. Cartling, *J. Phys. C* **8**, 3171 (1975).

²¹I. G. Austin, W. A. Jackson, T. M. Searle, P. K. Bhat, and R. A. Gibson, *Philos. Mag. B* **52**, 271 (1985).

²²E. O. Kane, *Solid-State Electron.* **28**, 3 (1985).

²³L. Ley, R. Karcher, and R. L. Johnson, *Phys. Rev. Lett.* **53**, 710 (1984).

²⁴N. F. Mott, *Metal-Insulator Transitions* (Taylor and Francis, London, 1974), p. 150.

²⁵H. Kurta, M. Hirose, and Y. Osaka, *Jpn. J. Appl. Phys.* **20**, L811 (1981).

²⁶H. P. Hjalmarson, H. Butner, and J. D. Dow, *Phys. Rev. B* **24**, 6010 (1981).

²⁷S. Fujita and A. Sasaki, *J. Electrochem. Soc.* **132**, 398 (1985).

²⁸G. Sasaki, M. Kondo, S. Fujita, and A. Sasaki, *Jpn. J. Appl. Phys.* **21**, 1394 (1982).